Journal Name

RSCPublishing

ARTICLE

The Unexpected Discovery of $Mg(HMDS)_2/MgCl_2$ Complex as Magnesium Electrolyte for Rechargeable Magnesium Batteries

Cite this: DOI: 10.1039/xoxxoooooox

Received ooth January 2012,
Accepted ooth January 2012

DOI: 10.1039/xoxxoooooox

www.rsc.org/

Chen Liao,* Niya Sa, Baris Key, Anthony Burrell, Lei Cheng, Larry Curtiss, John T. Vaughey, Jung-Je Woo, Libo Hu, Baofei Pan, Zhengcheng Zhang c

We developed a unique class of non-Grignard, aluminum-free magnesium electrolytes based on a simple mixture of magnesium compounds: magnesium hexamethyldisilazide ($Mg(HMDS)_2$) and magnesium chloride ($MgCl_2$). Through reverse Schlenk equilibrium, a concentrated THF solution of $Mg(HMDS)_2$-$4MgCl_2$ was prepared to achieve reversible Mg deposition/dissolution, a wide electrochemical window, and a coulombic efficiency of 99%. High reversible capacities and good rate capabilities were obtained in Mg–Mo_6S_8 cells using these new electrolytes in tests with different rates. The unexpected high solubility of $MgCl_2$ in the solvent of THF with the help from $Mg(HMDS)_2$ provides a new way to develop magnesium electrolytes.

Introduction

Rechargeable batteries are useful power sources for consumer electronics and electric vehicles. Lithium-ion batteries constitute the leading technology for such energy storage at present; however, concerns remain about cost and safety. Development of new rechargeable batteries with a high energy density and low cost requires new electrode and electrolyte materials that are cost-effective and environmentally benign. Magnesium is a very attractive anode due to its abundance (2.3 wt% in earth's crust), high theoretical specific capacity of 2205 Ah/kg, and high theoretical energy density of 3800 mAh/g.[1]

Development of magnesium-ion batteries[2, 3] faces two challenges: the lack of (i) high-energy-density cathodes that can intercalate Mg^{2+} and (ii) electrolytes that have reversible magnesium deposition/dissolution, and are compatible with a high voltage transition metal oxide cathode. Grignard reagents were reported as attractive magnesium electrolytes as early as 1917.[4] The ether solutions of the Grignard reagent allow reversible magnesium deposition/dissolution with high coulombic efficiency, but they have fairly low anodic stability with an electrochemical window usually less than 1.8 V.[5] By introducing a Lewis acid such as $AlCl_3$ or $AlCl_2Et$, the electrochemical window of the resulting organohaloaluminate electrolyte can be substantially increased.[6] One example is ($Mg(AlCl_2EtBu)_2$, Dichloro complex(DCC)), which has a reversible deposition/dissolution efficiency of almost 100% and an anodic stability up to 2.4 V vs Mg/Mg^{2+}.[7] Other magnesium electrolytes with improved safety and larger electrochemical window have also been reported. For example, a boron-based magnesium electrolyte has a high anodic potential of 3.5 V vs. Mg/Mg^{2+};[8] an amide-based magnesium electrolyte made from the crystal of $[Mg_2Cl_3(THF)_6]^+[HMDSAlCl_3]^-$ is both anodically stable and non-nucleophilic, with a reported anodic potential of 3.2 V vs. Mg/Mg^{2+};[9] and phenoxide-based and alkoxide-based magnesium electrolytes with anodic stability up to 2.5 V vs. Mg/Mg^{2+}.[8] Recently, an inorganic Mg-ion electrolyte consisting of only $MgCl_2$ and $AlCl_3$ has been reported to have an anodic potential approaching 3.3 V vs. Mg/Mg^{2+}.[10, 11]

A problem associated with these magnesium organohaloaluminate electrolytes is the inclusion of Lewis acids (boron[12] or aluminum substrates), which introduces a source of contamination. Avoidance of the Lewis acid has been demonstrated with a class of magnesium boron salts, $Mg(BH_4)_2$[13] and $Mg(C_2H_{12}B_{10})Cl$,[14] however, either narrow electrochemical window or synthetic difficulty might be a concern for this type of electrolytes.

In this article, we report a strategy to prepare a new electrolyte, the magnesium hexamethyldisilazide ($Mg(HMDS)_2$)/$MgCl_2$, which is non-pyrophoric, Lewis acid-free, yet keeps the same favorable properties of other magnesium organohaloaluminates, including the high solubility (up to 1.25 M [Mg^{2+}]), high ionic conductivity, wide electrochemical window, and excellent electrochemical reversibility. The HMDS group has been introduced into the 3(HMDS)MgCl-$AlCl_3$ complex,[9] however, coordination with the anion $(HMDS)AlCl_3^-$ (as shown in the crystal structure), as well as several steps of air-free syntheses and further purification such as recrystallization were required for its high electrochemical performance. In contrast, the new discovered $Mg(HMDS)_2$/$MgCl_2$ electrolyte is easy to prepare: the synthesis can be carried out by simply mixing the two commercial salts of $Mg(HMDS)_2$ and $MgCl_2$, without usage of any Schlenk Line or purification technique.

Results and Discussion

Through the preparation of the $Mg(HMDS)_2$/$MgCl_2$ electrolyte, the $MgCl_2$ salt showed significantly enhanced solubility in the mixture of $Mg(HMDS)_2$-THF . In a solubility control test, the $MgCl_2$ salt alone shows little or no solubility in the THF solvent, however, in the presence of 0.25 M $Mg(HMDS)_2$, the solubility of the $MgCl_2$ salt in the THF is enhanced dramatically, even reaching up to 1 M upon substantially stirring. We attributed the enhanced solubility of $MgCl_2$ in THF to the mechanism that reverses Schlenk equilibrium (Scheme 1a): the $Mg(HMDS)_2$ is a covalent-bonded magnesium complex while the $MgCl_2$ is an ionic-bonded species. By mixing them in an organic solvent (Scheme 1b), ligands exchange rapidly, and new species suitable for magnesium-ion batteries are generated.

One advantage of the new $Mg(HMDS)_2$ /$MgCl_2$ electrolyte is that, it is also easy to tune the parameters such as the ratio of $Mg(HMDS)_2$/$MgCl_2$ and the type of the solvents in the new electrolyte. Another important finding is that an excess amount of $MgCl_2$ (3 or more equivalents relative to $Mg(HMDS)_2$) has to be present to introduce new chemistry including the reversed Schlenk equilibrium. Through both experimental observation and simulation results, the new chemistry of the pivotal role of $MgCl_2$ in assisting the formation of active species such as $(HMDS)MgCl_2^-$ and $Mg_2Cl_3^+$ was proposed. Through experimental observation of the candidates, the $Mg(HMDS)_2$–$n$$MgCl_2$/THF ($n \geq 3$) mixture has the best anodic stability, ionic conductivity, and diffusion properties.

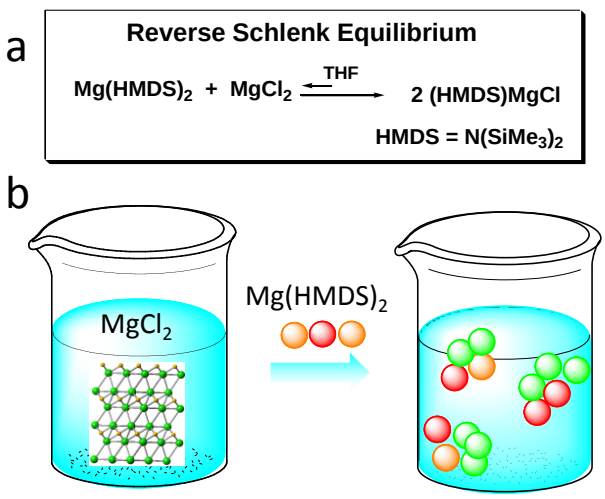

Scheme 1. (a) Schematic representation of the reverse Schlenk equilibrium for designing new magnesium electrolyte. (b) Schematic illustration of how $Mg(HMDS)_2$ facilitates the solvation of $MgCl_2$ in THF.

The structures of the $Mg(HMDS)_2$ /$MgCl_2$ electrolyte were also studied and analyzed by nuclear magnetic resonance (NMR) spectroscopy. As was mentioned early, the new $Mg(HMDS)_2$/$MgCl_2$ electrolyte was prepared by stirring commercially available $Mg(HMDS)_2$ and $MgCl_2$ salts in the THF solvent under an inert atmosphere until the two salts completely dissovled. The formation of new components inside the electrolyte of the $Mg(HMDS)_2$/$MgCl_2$ was confirmed by ^1H, ^{13}C, and ^{25}Mg NMR (Figure 1). Through a separate experiment, the pure $Mg(HMDS)_2$ in THF with D_2O capillary (used as deuterium-lock) exhibits a signal with a chemical shift of -0.032 ppm in ^1H NMR and 5.7 ppm (quartet, Figure 1, set of b in ^{13}C NMR) in ^{13}C NMR spectra and was assigned to the CH_3 group of $Mg(HMDS)_2$. After $MgCl_2$ was dissolved with $Mg(HMDS)_2$, other than the signals in the ^1H and ^{13}C NMR spectra that are the same as those of $Mg(HMDS)_2$, a new signal was observed with a chemical shift of 0.007 ppm in ^1H NMR and 6.3 ppm (quartet, Figure 1, set of a in ^{13}C NMR) in ^{13}C NMR spectra. This finding confirms the formation of a new species in the reaction between $Mg(HMDS)_2$ and $MgCl_2$. Furthermore, three signals with chemical shifts at 8.1, 4.4, and -0.4 ppm were obtained from the deconvolution of the ^{25}Mg NMR signal (Figure 1, right) indicating the formation of new magnesium ion species.

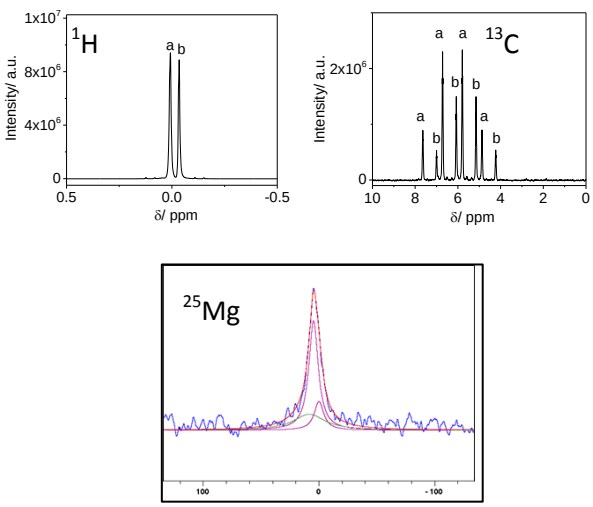

Figure 1. ^1H, ^{13}C, and ^{25}Mg NMR spectra of $Mg(HMDS)_2$/$4MgCl_2$-THF solution.

Based on the NMR spectroscopy data, the new Mg-ion species in the electrolyte consists of H, Si, and Mg. Density functional theory (DFT) modeling data indicates the existence of the $[(HMDS)MgCl_2]^-$ anion and the formation of the $[(HMDS)MgCl_2$-$Mg_2Cl_3]$ complex as shown in Scheme 2. The free energy of each reaction step was calculated by DFT to evaluate the thermodynamic feasibility of the reaction sequence (Fig.S1 in supporting information). As shown in Eqn (1), the reverse Schlenk equilibrium between $Mg(HMDS)_2$ and $MgCl_2$ yields the intermediate (HMDS)MgCl. The free energy calculated for this reaction is −0.39 eV. As shown in Eqn (2), the transmetallation between (HMDS)MgCl and $MgCl_2$ yields the [(HMDS)$MgCl_2$-MgCl] complex, and this reaction is exothermic by 0.26 eV. As shown in

Eqn (3), the [(HMDS)$MgCl_2$-MgCl] complex can further react with $MgCl_2$ and forms [(HMDS)$MgCl_2$-Mg_2Cl_3] as the final product, and the reaction is exothermic by -0.38 eV. Given the free energies calculated for the possible reactions, the reaction shown in Scheme 2 and the pathway shown in Figure S1 (black arrow) is the most favorable. Isolation of a single crystal from the $Mg(HMDS)_2/MgCl_2$ electrolyte would be helpful for the identification of the new species; however, $Mg(HMDS)_2/MgCl_2$ tends to precipitate out of the solution with no formation of a single crystal.

$Mg(HMDS)_2 + MgCl_2 \rightarrow 2\ (HMDS)MgCl$ Eq. (1)

$(HMDS)MgCl + MgCl_2 \rightarrow [(HMDS)MgCl_2\text{-}MgCl]$ Eq. (2)

$[(HMDS)MgCl_2\text{-}MgCl] + MgCl_2 \rightarrow [(HMDS)MgCl_2\text{-}Mg_2Cl_3]$ Eq. (3)

Scheme 2. Proposed chemical reactions of the THF solution of $Mg(HMDS)_2/4MgCl_2$ toward the desired structure of $[Mg_2Cl_3(THF)_6]^+[(HMDS)MgCl_3]$ as revealed by DFT calculation.

Fundamental electrochemical properties of this new electrolyte were then performed including ionic conductivity, diffusion coefficient, metal deposition/dissolution and electrochemical stability. Two parameters were varied to optimize the electrolytic properties: the ratio between $Mg(HMDS)_2$ and $MgCl_2$ and their concentrations. Based on Scheme 2, the stoichiometric ratio of the $Mg(HMDS)_2$ and $MgCl_2$ to form the proposed (HMDS)$MgCl_2$-Mg_2Cl_3 would be 1:3. Our experimental results are in good agreement with this prediction, furthermore, increase of the amount of $MgCl_2$ maintained the good electrochemical performance. Recently, Aurbach *et al* reported that a "conditioning" process is essential for $MgCl_2$-$AlCl_3$ type electrolyte[10] to provide stable electrochemical performance, while Gewirth group reported that activation CV cycles[11] are required for $MgCl_2$-$AlCl_3$ type electrolyte to obtain a high coulombic efficiency. For the new $Mg(HMDS)_2/MgCl_2$ electrolyte, no extra conditioning or activation CV cycles is needed for the good electrochemical performance.

The magnesium deposition and dissolution were measured by cyclic voltammetry using $Mg(HDMS)_2/MgCl_2$ electrolytes with different ratios. The examined electrolytes are: $2Mg(HMDS)_2$–$MgCl_2$/THF, $Mg(HMDS)_2$–$2MgCl_2$/THF and $Mg(HMDS)_2$–$4MgCl_2$/THF. For simplicity, the concentration of the salt used in this paper always refers to the concentration of all the Mg^{2+} species in the solution,for example, a 0.5 M $2Mg(HMDS)_2$–$MgCl_2$ comprises of 0.33 M $Mg(HMDS)_2$ and 0.17 M $MgCl_2$. The $Mg(HMDS)_2$-$3MgCl_2$ solution showed good electrochemical behavior (Figure S3). Compared to the $Mg(HMDS)_2$-$3MgCl_2$ solution, the $Mg(HMDS)_2$-$4MgCl_2$ solution has one excess stoichiometric amount of $MgCl_2$ and shows even more stable performance, therefore, it was selected as the "workhorse" electrolyte in this work. Figure 2 shows the cyclic voltammograms for 0.5 M $Mg(HMDS)_2$-$4MgCl_2$/THF solutions together with other electrolytes with different $Mg(HMDS)_2$ and $MgCl_2$ ratios. All the electrolyte mixtures showed reversible Mg deposition/dissolution. With an increasing amount of $MgCl_2$, the electrochemical window broadens significantly from 2.3 V, 2.75 V, and 2.8V for $2Mg(HMDS)_2$-$MgCl_2$, $Mg(HMDS)_2$-$2MgCl_2$ and $Mg(HMDS)_2$-$4MgCl_2$, repectively. The coulombic efficiency (CE) of the Mg dissolution/deposition also improves when the content of $MgCl_2$ increases. For the electrolytes with $Mg(HMDS)_2$ and $MgCl_2$ ratios at 2:1, 1:2, and 1:4, the CE was 85%, 95%, and 99%, respectively, suggesting a highly efficient and reversible Mg deposition/dissolution process for the $Mg(HMDS)_2$-$4MgCl_2$ electrolyte. The high ratio $Mg(HMDS)_2$ an $MgCl_2$ elelctrolyte also showed redution in overpotential. It decreases from -0.41 V for $2Mg(HMDS)_2$–$MgCl_2$/THF to -0.24 V for $Mg(HMDS)_2$–$4MgCl_2$/THF. Apparently, the addition of $MgCl_2$ enhances the anodic stability and mitigates the overpotential for Mg deposition.

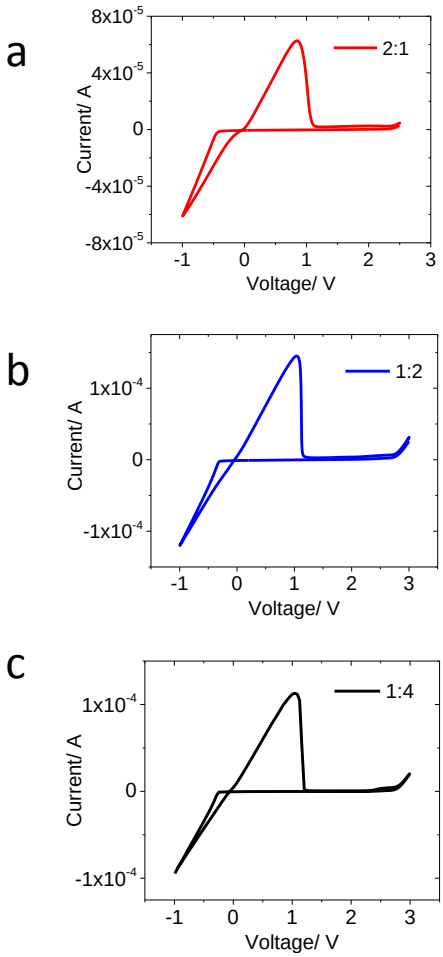

Figure 2. Typical cyclic voltammograms with Pt electrodes of THF solution containing $Mg(HMDS)_2$ and $MgCl_2$ at different ratios: (a) 0.5 M $2Mg(HMDS)_2$–$MgCl_2$/THF, (b) 0.5 M $Mg(HMDS)_2$–$2MgCl_2$/THF, (c) 0.5 M $Mg(HMDS)_2$–$4MgCl_2$/THF. The scan rate is 100 mV s^{-1} with Pt as working electrode and Mg ribbons as both reference and counter electrode.

Figure 3 shows the cyclic voltammograms of $Mg(HDMS)_2$-$4MgCl_2$ with different concentrations in THF solvent. Deposition and dissolution of Mg were clearly observed at concentrations of 0.25–1.25 M; however, the current decreases significantly at lower electrolyte concentrations. For instance, the cathodic and anodic current decreases over 50 times as the concentration of $Mg(HDMS)_2$-$4MgCl_2$/THF decreases by five times, from 1.25 M to 0.25 M. This result suggests that, in the $Mg(HDMS)_2$-$4MgCl_2$/THF, the concentration of Mg^{2+} plays a crucial role in triggering the deposition of Mg at the surface of the working electrode.

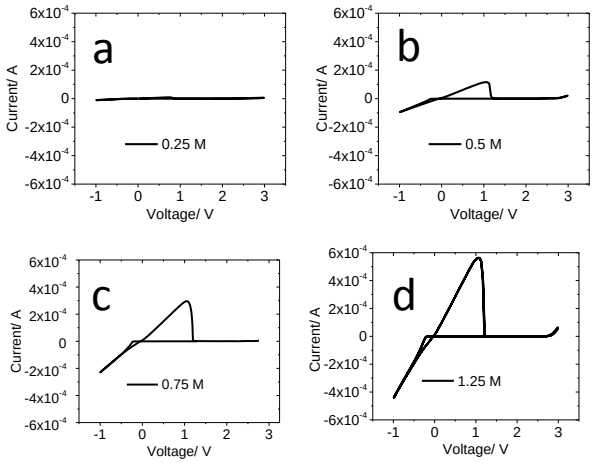

Figure 3. Typical cyclic voltammograms of THF solutions containing $Mg(HMDS)_2$-$4MgCl_2$ at different concentrations. The scan rate is 100 mV s^{-1}, and Pt was used as the working electrode (Φ = 2 mm) with a Mg ribbon as both and counter electrodes.

The cyclic voltammograms of the $Mg(HDMS)_2$-$4MgCl_2$ in different solvents including dimethoxyethane (DME), diethylene glycol dimethyl ether (diglyme), and tetraethylene glycol dimethyl ether (tetraglyme) were illustrated in Fig. S2.The addition of THF to the glyme-based electrolytes improves the solubility of $Mg(HDMS)_2$-$4MgCl_2$ in the glymes. However, reversible magnesium deposition/dissolution with good efficiency was only observed in DME electrolyte with addition of THF. A possible explanation is that the chelating effect of diglyme, triglyme, and tetraglyme might create a strong solvation sheath around magnesium ions and thus prevents Mg deposition. Recently it is demonstrated that Mg ion association strongly depends on the solvent,[15] and the ion association reduces the effective charge of the solvated cation, as well as influences the desolvation of the cation at the electrolyte/electrode interphase. Further study is in progress for the solvation sheath of these magnesium electrolytes by NMR and Pair Distribution Function (PDF).

To determine the morphology and the composition of the deposited Mg species, several hundred microns of Mg was deposited on a Pt working electrode from the 0.5 M THF solution of $Mg(HMDS)_2$-$4MgCl_2$. The scanning electron micrographs in Figure 4a show evenly distributed particles with size ranging from *ca.* 50 to 200 µm, much larger than those observed in the $MgCl_2$-$AlCl_3$ solutions.[8] Figure 4b depicts the fine layers observed from the edges of the deposited Mg metal, and clearly, the Mg atom deposited in a layered fashion on the electrode surface. Energy dispersive X-ray spectroscopy analysis (EDS) confirmed that the Mg metal was deposited free from Al contamination.. The absence of any other species confirms the unique property of the new $Mg(HMDS)_2/MgCl_2$ electrolyte.

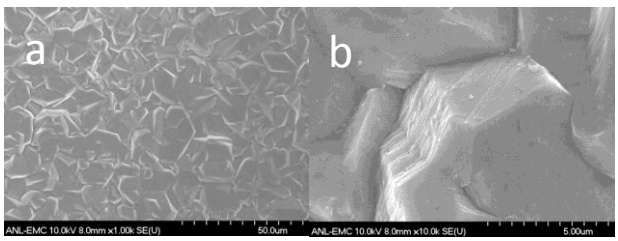

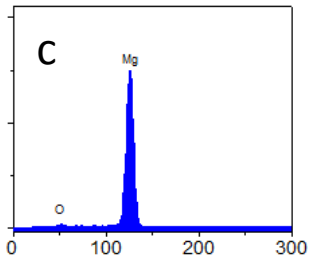

Figure 4. SEM images of the deposited Mg on a Pt working electrode at 50.0 µm (a) and 5.00 µm resolutions (b). The EDS spectrum (c) recorded for the deposited Mg on a Pt working electrode from a 0.5 M THF solution of $Mg(HMDS)_2$-$4MgCl_2$. The O peak results from oxidation of Mg metal during the exposure to air.

Study of the diffusion and transport properties in the non-aqueous electrolytes is important since it provides a better understanding of the mass transport property and can serve as a criterion for the electrolyte performance. Figure 5 shows the temperature dependence of the ionic conductivity of $Mg(HMDS)_2$-$4MgCl_2$/THF. For the 0.25 M $Mg(HMDS)_2$-$4MgCl_2$/THF, the ionic conductivity was low, in the range of 0.03–0.04 mS cm^{-1}, and is not sensitive to the temperature. However, when the concentration increased, the conductivity increased significantly especially at high temperatures. For example, the conductivity at 10 °C increased from 0.03 mS cm^{-1} to 0.17 mS cm^{-1} when the concentration increased to 0.5 M; Further increase of the concentration, from 0.5 M to 0.75 M, the ionic conductivity increased significantly (from 0.017 to 0.5 mS cm^{-1}). The conductivity increased dramatically when the temperature is elevated tot 60 °C, from 0.04 mS cm^{-1} for 0.25 M to 0.9 mS cm^{-1} for 0.75 M concentration .

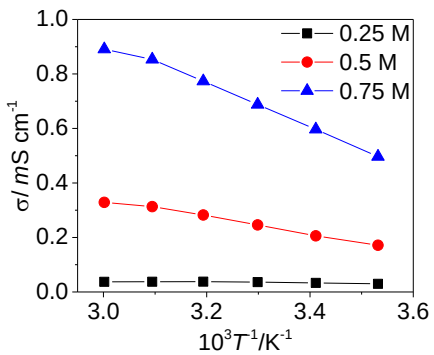

Figure 5. Temperature dependence of ionic conductivity at different $Mg(HMDS)_2$-$4MgCl_2$/THF concentrations.

The $Mg(HMDS)_2/MgCl_2$ electrolyte has fairly complex diffusion properties and through our experiment, it does not exhibit a linear correlation between the faradaic current and the scan rate. Therefore, the diffusion coefficient of $Mg(HMDS)_2/MgCl_2$ can not be estimated by a simple Randles-Sevcik analysis which compares the cyclic voltammograms at different scan rates. To evaluate the effect of the cation diffusion coefficients of the $Mg(HMDS)_2/MgCl_2$ electrolyte, a negative potential of - 0.5 V vs. Mg/Mg^{2+} was applied on the Pt working electrode and Mg deposited on the working electrode. Depletion of the cation species (Mg^{2+}) near the electrode surface leads to an inverse relationship of $t^{1/2}$, and this trend is an indication of a diffusion-controlled process.[16] The rate of

how fast cations can diffuse next to the electrode surface is concentration dependent, as shown in Figure 6. Charge density increases as the electrolyte concentration increases (Figure 6a), and as a consequence, the diffusion coefficient increases. As shown in Figure 6b, the diffusion coefficient increases nearly three orders of magnitude, from 6.3×10^{-10} cm^2/s at 0.25 M to 1.0×10^{-7} cm^2/s at 1.25 M. This trend could explain why the electrochemical performance of MgHDMS-4$MgCl_2$/THF is better at higher electrolyte concentrations. The diffusion coefficient for solutions with concentrations of 0.5 to 1.25 M is in the range of 3×10^{-8} to 10^{-7} cm^2/s, which is in the same range as reported for the magnesium organohaloaluminate electrolyte C_2H_5MgCl-$(C_2H_5)_2AlCl_2$.[16] A distinguishing feature of the $Mg(HMDS)_2/MgCl_2$ electrolyte is that diffusion increases as the concentration increases, while for C_2H_5MgCl-$(C_2H_5)_2AlCl_2$ electrolyte, the diffusion decreases as the concentration increases.[16]

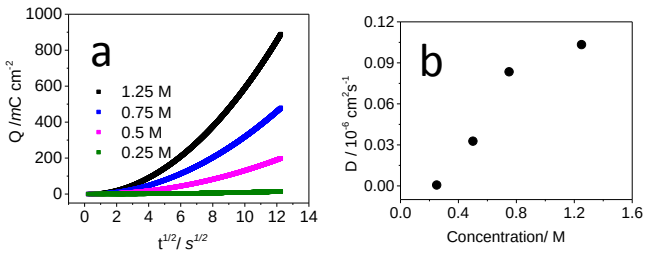

Figure 6. Measured diffusion coefficient of Mg ion as a function of $Mg(HMDS)_2$-4$MgCl_2$/THF concentration at room temperature.

The Chevrel phase Mo_6S_8 is an efficient Mg-ion cathode material with reported reversible intercalation/de-intercalation of Mg ion over thousands of cycles.[7] We synthesized the Mo_6S_8 following a literature procedure[17] to evaluate the reversibility of the new $Mg(HMDS)_2/MgCl_2$ electrolytes. Because of the improved safety of the new $Mg(HMDS)_2/MgCl_2$ electrolyte as compared to the other Grignard-based electrolytes, the 2032 coin cells with the new electrolyte can be tested at 55 °C. as high temperature cycling overcomes the slow kinetics of Mo_6S_8.[18] . Figure 7a shows the typical discharge–charge voltage profiles of the Mg–Mo_6S_8 cell at a current rate of 0.1 C using an electrolyte of 0.5 M $Mg(HDMS)_2$-4$MgCl_2$/THF at 55 °C. Two typical discharge plateaus at 1.23 V and 1.1 V were observed. Figure 7b showed the cycling performance. The Mo_6S_8 electrode exhibits a reversible discharge capacity of 86 mAh g^{-1}, indicating that the new $Mg(HDMS)_2/MgCl_2$ electrolyte can be successfully used in rechargeable Mg batteries. A slight capacity loss after 30 cycles may originate from the gradual evaporation of THF solvent at 55°C. The Mg–Mo_6S_8 cell with a 0.5 M $Mg(HDMS)_2$-4$MgCl_2$/THF electrolyte also shows good rate capability at 55 °C (Figures 7c and 7d). These results confirmed the excellent performance of the new $Mg(HDMS)_2/MgCl_2$ electrolyte in Mg-ion rechargeable batteries.

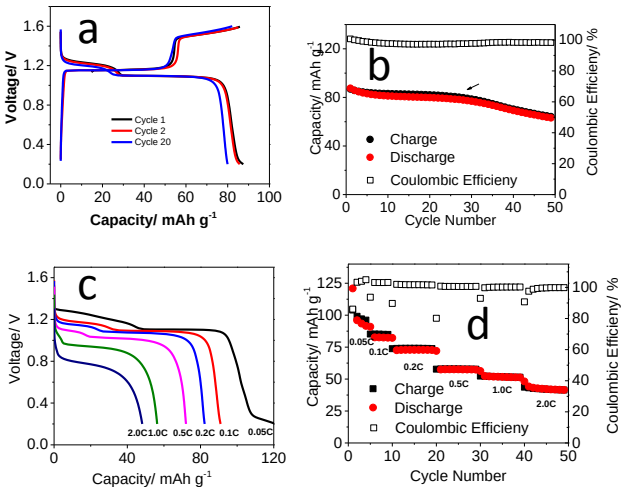

Figure 7. Discharge/charge voltage profile (a) and cycling performance (b) of the Mg–Mo_6S_8 cells at a current rate of 0.1 C in 1.25 M $Mg(HMDS)_2$-4$MgCl_2$/THF electrolyte at 55 °C. Typical discharge curves of the Mg–Mo_6S_8 cells in 1.25 M $Mg(HMDS)_2$-4$MgCl_2$/THF electrolyte at different current rates and 55 °C (c); typical rate performance and corresponding coulombic efficiencies at a current rate of 0.1, 0.2, 0.5, 1, and 2 C and 55 °C (d).

Conclusions

In sum, the reverse Schlenk equilibrium mechanism (Scheme 1) resulted in the development of a novel magnesium electrolyte ($Mg(HMDS)_2/MgCl_2$) with improved coulombic efficiency and electrochemical window. The success key of the invention of this $Mg(HMDS)_2/MgCl_2$ is the superior solubility of $MgCl_2$ in THF in the presence of $Mg(HMDS)_2$. The reverse Schlenk equilibrium mechanism can also be applied to a variety of materials, including amides and many other covalently bonded magnesium salts. The excellent electrolytic properties of the new $Mg(HMDS)_2$-$MgCl_2$ complex were demonstrated and the new electrolyte was successfully cycled as electrolyte in a Mg-Mo_6S_8 coin cell. It is also surprising that the electrochemical, diffusion, and transport properties closely depend on $Mg(HMDS)_2$-4$MgCl_2$/THF concentration and also on the ratio between the magnesium amide and the magnesium chloride. Analytical methods such as NMR spectroscopy and DFT theoretical calculation confirmed the formation of a new species in the magnesium amide/magnesium chloride mixture. Future studies will focus on the Mg solvation structure in the electrolyte and the development of other new magnesium electrolytes.

Acknowledgements

This work was supported as part of the Joint Center for Energy Storage Research, an Energy Innovation Hub funded by the U.S. Department of Energy, Office of Science, Basic Energy Sciences. The submitted manuscript has been created by UChicago Argonne, LLC, Operator of Argonne National Laboratory (“Argonne”). Argonne, a U.S. Department of Energy Office of Science laboratory, is operated under Contract no. DE-AC02-06CH11357. The electron microscopy was

accomplished at the Electron Microscopy Center at Argonne National Laboratory.

Notes and references

[a] Joint Center for Energy Storage Research; Argonne National Laboratory, Lemont, Illinois, USA

† Footnotes should appear here. These might include comments relevant to but not central to the matter under discussion, limited experimental and spectral data, and crystallographic data.
Electronic Supplementary Information (ESI) available: [details of any supplementary information available should be included here]. See DOI: 10.1039/b000000x/

1 H. D. Yoo, I. Shterenberg, Y. Gofer, G. Gershinsky, N. Pour and D. Aurbach, *Energy Environ. Sci.*, 2013, **6**, 2265-2279.
2. I. Shterenberg, M. Salama, Y. Gofer, E. Levi and D. Aurbach, *MRS Bulletin*, 2014, **39**, 453-460.
3. I. Shterenberg, M. Salama, Y. Gofer, E. Levi and D. Aurbach, *MRS Bulletin*, 2014, **39**, 453-460.
4. J. M. Nelson and W. V. Evans, *J. Am. Chem. Soc.*, 1917, **39**, 82-83.
5. L. P. Lossius and F. Emmenegger, *Electrochim. Acta*, 1996, **41**, 445-447.
6. D. Aurbach, H. Gizbar, A. Schechter, O. Chusid, H. E. Gottlieb, Y. Gofer and I. Goldberg, *J. Electrochem. Soc.*, 2002, **149**, A115-A121.
7. D. Aurbach, Z. Lu, A. Schechter, Y. Gofer, H. Gizbar, R. Turgeman, Y. Cohen, M. Moshkovich and E. Levi, *Nature*, 2000, **407**, 724-727.
8. F.-f. Wang, Y.-s. Guo, J. Yang, Y. Nuli and S.-i. Hirano, *Chem. Comm.*, 2012, **48**, 10763-10765.
9. Y.-S. Kim, T.-H. Kim, H. Lee and H.-K. Song, *Energy & Environmental Science*, 2011, **4**, 4038-4045.
10. R. E. Doe, R. Han, J. Hwang, A. J. Gmitter, I. Shterenberg, H. D. Yoo, N. Pour and D. Aurbach, *Chem. Comm.*, 2014, **50**, 243-245.
11. C. J. Barile, R. Spatney, K. R. Zavadil and A. A. Gewirth, *J. Phys. Chem. C*, 2014, **118**, 10694-10699.
12. T. D. Gregory, R. J. Hoffman and R. C. Winterton, *J. Electrochem. Soc.*, 1990, **137**, 775-780.
13. R. Mohtadi, M. Matsui, T. S. Arthur and S.-J. Hwang, *Angew. Chem. Int. Ed.* , 2012, **51**, 9780-9783.
14. T. J. Carter, R. Mohtadi, T. S. Arthur, F. Mizuno, R. Zhang, S. Shirai and J. W. Kampf, *Angew. Chem. Int. Ed.* , 2014, **53**, 3173-3177.
15. S. H. Lapidus, N. N. Rajput, X. Qu, K. W. Chapman, K. A. Persson and P. J. Chupas, *PCCP*, 2014.
16. A. Benmayza, M. Ramanathan, T. S. Arthur, M. Matsui, F. Mizuno, J. Guo, P.-A. Glans and J. Prakash, *J. Phys. Chem. C*, 2013, **117**, 26881-26888.
17. E. Lancry, E. Levi, A. Mitelman, S. Malovany and D. Aurbach, *J. Solid State Chem.*, 2006, **179**, 1879-1882.
18. C. Liao, B. Guo, D.-e. Jiang, R. Custelcean, S. M. Mahurin, X.-G. Sun and S. Dai, *J. Mater. Chem. A*, 2014, **2**, 581-584.

